Reassessment of source parameters for three major earthquakes in the East African rift system from historical seismograms and bulletins

Atalay Ayele ([1])([2]) **and Ota Kulhánek** ([1])

([1]) *Department of Earth Sciences, Seismology, Uppsala University, Uppsala, Sweden*

([2]) *Geophysical Observatory, Science Faculty, Addis Ababa University, Addis Ababa, Ethiopia*

Abstract

Source parameters for three major earthquakes in the East African rift are re-computed from historical seismograms and bulletins. The main shock and the largest foreshock of the August 25, 1906 earthquake sequence in the main Ethiopian rift are re-located on the eastern shoulder of the rift segment. The magnitude of the main shock is estimated to be 6.5 (M_w) from spectral analysis. The December 13, 1910 earthquake in the Rukwa rift (Western Tanzania) indicated a significant strike-slip component from teleseismic body-waveform inversion for fault mechanism and seismic moment. The January 6, 1928 earthquake in the Gregory rift (Kenya) showed a multiple rupture process and unusually long duration for a size of 6.6 (M_w). The May 20, 1990 earthquake in Southern Sudan, mentioned merely for the sake of comparison, is the largest of all instrumentally recorded events in the East African rift system. Despite the fact that the mode of deformation in the continental rift is predominantly of extensional nature, the three largest earthquakes known to occur in the circum-Tanzanian craton have shallow focal depths and significant strike-slip component in their fault mechanisms. This and similar works will enrich the database for seismic hazard assessment in East Africa.

Key words *East African rift system – fault mechanisms – seismic hazard – source parameters*

1. Introduction

Significant earthquakes in the East African rift have caused relatively less damage and loss of life compared to similar earthquakes in other earthquake prone regions. This difference in earthquake damage is mainly due to the low level of economic development and sparse population distribution. Currently, urbanisation and development projects are rapidly growing in number and existing towns are expanding in size. Such new developments imply increasing earthquake vulnerability of engineering structures and population centres. Therefore, to minimise the effect of future damaging earthquakes in the East African region, a sound seismic hazard assessment and earthquake effect mitigation program is vital.

Seismotectonic consideration in the region with data starting from as far back in time as possible is important for seismic hazard study. A reliable seismic hazard assessment of an area integrates a wide range of geological and paleoseismological data in addition to historical and instrumental seismicity. Geologic and paleoseis-

Mailing address: Dr. Atalay Ayele, Department of Earth Sciences, Seismology, Uppsala University, Villavägen 16, S-752 36, Uppsala, Sweden; e-mail: atawon@yahoo.com

mic information provides quantitative data on major earthquakes in the past that can be used directly or indirectly in seismic hazard analysis. However, this is currently possible only in a few countries like, for instance, Japan, China, Italy and Greece, which have a long recorded earthquake history and are capable of conducting a wide spectrum of geological and geophysical investigations. In East Africa, there is little or no historical seismic data and the quality of instrumental earthquake data is poor. Paleoseismic evidence which needs extensive work and caution in interpretation and practical applications (Valensise, 1995) is a task for the future.

Among the most important data in geophysics are the seismograms which produce most of the basic and quantitative information concerning the seismic source and the Earth's interior (Kanamori, 1988). Source dynamics of earthquakes with magnitude as small as 0.5 (M_L) have been determined using currently achieved techniques and instrumentation (*e.g.*, Rögnvaldsson and Slunga, 1993). On the other hand, historical seismograms and bulletins from significant earthquakes of magnitude $M \sim 7.0$ (M_s) have not been fully exploited except for classical arrival-time readings. This is because the new theories and methods were not well developed by then; hence the available data could not be interpreted fully.

The years just preceding the relatively higher development of seismometry in the early 1960s were periods of greater seismic activity in East Africa than the years that followed (Gutenberg and Richter, 1954). The earthquake catalogue of the East African region shows that, with the exception of the 1990 Southern Sudan event, most of the significant earthquakes in the region occurred during the first half of this century. Source parameter estimates of some of the earlier earthquakes are uncertain due to under-developed instrumentation, computational techniques and extremely sparse world-wide station distribution prior to the 1960s. Even the events already located in ISS/ISC (International Seismological Summary/International Seismological Centre) catalogues are under scrutiny using new techniques and global earth models (Engdahl, 1997; Shedlock *et al.*, 1997), which shows remarkable differences with the previous seismicity for some test areas. It is therefore important to extract all possible information of the pre-WWSSN earthquakes from historical bulletins and seismograms to enrich the database on which seismic hazard assessment is to be based.

Three major historical earthquakes are considered for reassessment of source parameters in the present study. These are the August 25, 1906 (Ethiopia), December 13, 1910 (Tanzania) and January 6, 1928 (Kenya) earthquakes. The May 20, 1990 earthquake in Southern Sudan is cited only for comparison.

The province of Shoa in Ethiopia was subjected to a severe earthquake sequence from August 25 to November 8, 1906 (Gouin, 1979). The main shock on August 25 ($M_s = 6.8$) is the largest of this century recorded in the country and was widely felt. It is the first instrumentally well-recorded event of the pre-1960 era by the then low-gain and band-limited instruments. Stations as far away as Osaka (Japan), Australia, Argentina, and British Columbia (seismological bulletins, Ambraseys and Adams, 1991) recorded this event. Limited macroseismic information was also available from nearby towns like Addis Ababa, Adamitullu and Lake Langano areas with increasing intensity southwards (fig. 1). None of the macroseismic reports give any specific time of the observation. The accuracy of timing was poorly known in Africa at the beginning of this century. All the available macroseismic data were used to locate the main shock of 1906. However, the macroseismic data would probably be influenced by one of the many possible earthquakes of this sequence or other secondary phenomena like site effects and associated landslides. These uncertainties together will make the accuracy of the location based on macroseismic data alone less reliable.

About two hours before the rupture of the main shock, there was one larger identified foreshock at around 11 h 54 min which was recorded with clear *P* and *S* phases at teleseismic distances. This event is amenable for location with few limitations due to possible mis-identification of phases. The *S* arrival-time at TIF (Tiflis, Georgia) station, for instance, was reported as a *P* arrival-time. This foreshock was located at the same site as the main shock by

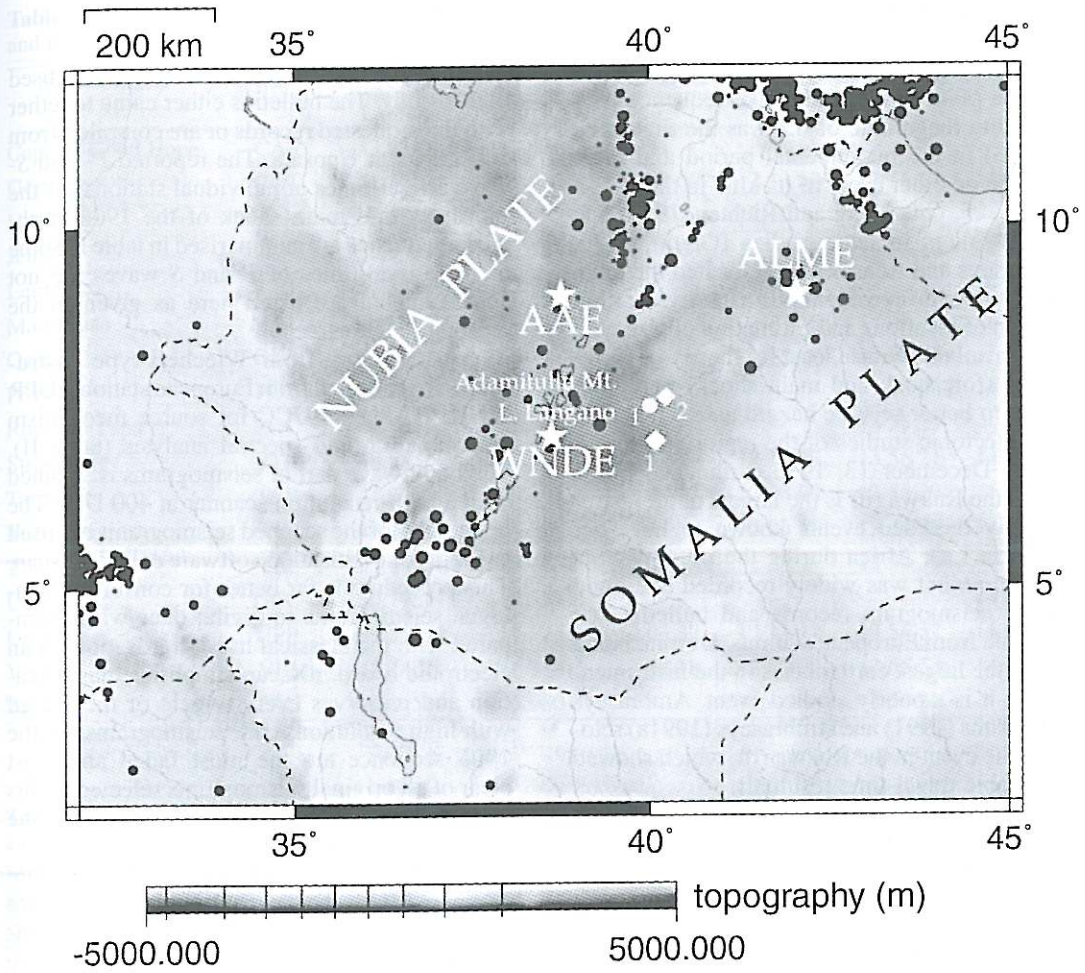

Fig. 1. Seismicity of the main Ethiopian rift starting from the turn of this century until 1993. Earthquakes with specified location but without magnitude estimate from Gouin (1979) for the time prior to 1960 and Ayele (1995) catalogues are assigned a value of 2.0 and 4.0, respectively, to mark them on the map. The shading represents topography and the dark area corresponds to the Ethiopian plateaus. The white stars are permanent seismic stations currently operating in Ethiopia. White diamonds are the epicenters of the foreshock (2) and main shock (1) of the 1906 earthquake sequence determined in this study. The white circle marks the location of the main shock (1) after Ambraseys and Adams (1991).

Gutenberg and Richter (1954). Besides these two events, which were clearly recorded by many distant stations, five more were felt around Adamitullu mountain (fig. 1) in the afternoon of the same day. Arrival-times of *L* (Large wave) and *M* (Maximum wave) phases for two events at TIF, one event at UPP (Uppsala, Sweden) and HAM (Hamburg, Germany) stations were reported on August 25, 1906 after the main shock. There were no corresponding reports from bulletins of other stations. These could probably be two of the larger aftershocks of the sequence.

The whole rupture process released significant stress energy in the main Ethiopian rift as a result of the extension between the Nubia and Somalia plates. This earthquake sequence with maximum magnitude of 6.5 was the first to be recorded in the instrumental period and there has been no other event of its kind in the region since 1906. Gutenberg and Richter (1954) and other workers in later studies (Gouin, 1979; Ambraseys and Adams, 1991) located the main event but with considerable disparity. Further revision of locations and estimation of size with all the available data at least for these two earthquakes (foreshock and main shock) may contribute to better seismic hazard assessment and seismotectonic studies of the region.

The December 13, 1910 earthquake (M_s = 7.3) in the Rukwa rift is the largest of all instrumentally recorded events known to have occurred in East Africa during the pre-WWSSN era. This event was widely recorded and good quality seismogram records and bulletins are available from European stations. Despite being one of the largest earthquakes in the instrumental era, it is a poorly studied event. Ambraseys and Adams (1991) and Ambraseys (1991a) relocated the event in the Rukwa rift, which showed reasonable travel-time residuals.

The 1928 Sabukia valley earthquake is the earliest and largest (M_s = 6.9) shock in the Gregory rift (Ambraseys, 1991b) to be well recorded instrumentally. It was not, however, the largest event in the whole of East Africa as suggested by Doser and Yarwood (1991). The source mechanism of this earthquake was studied by Doser and Yarwood (1991) and the results seem to be supported by field observations but the source-time function is assumed to be a simple step function and the whole inversion process is not well resolved. Seismogram records with good signal-to-noise ratio are available to us only from UPP and MNH.

Size estimates of these three earthquakes as given by Gutenberg and Richter (1954) are doubtful due to the inherent problem of their techniques and quality of data (Geller and Kanamori, 1977). Earthquake source parameters of these historical earthquakes are estimated using various techniques on the available data, taking note of their quality.

2. Data sources

Station bulletins and seismograms are used in this study. The bulletins either came together with the requested records or are compiled from collections at Uppsala. The reported *P*- and *S*-wave arrival-times at individual stations for the foreshock and main shock of the 1906 earthquake sequence are summarised in table I. Some of the arrival-times of *P* and *S* waves are not consistent but are listed here as given in the original bulletins.

Seismograms from Wiechert-type instruments are collected from European stations: UPP, MNH, HAM and UCC for source mechanism determination and spectral analysis (table II). The body-wave part of seismograms is scanned with a high-resolution scanner at 400 DPI. The image files of the scanned seismograms are used as input for digitisation software called nXscan. This procedure is far better for converting analogue seismograms to digital ones when compared with the classical hand digitisation on an electronic board. nXscan simplifies magnification and preserves every wiggle of the record with high resolution. UPP seismograms for the 1906 sequence are the most faded and least clear of all original seismograms selected in this study. The two horizontal components of the UPP station records for the main shock are displayed in fig. 2. The digitised seismograms are compared with the original ones and they are almost the same. It was possible to pick additional phases from the digital data, which have never been included in the original bulletin and hence used in the location procedure. Available seismograms from four stations (table II) are digitised at 1 Hz sampling frequency for all the events studied.

3. Method and analysis

Earthquake location, spectral analysis and waveform inversion for source mechanism determination and seismic moment (M_0) are employed in this study. Several stations are used for the event location (table I) while only four stations are available for waveform analysis.

Table I. Arrival-times bulletin from data archives of some of the then operating stations for the 1906 foreshock and main shock in the main Ethiopian rift.

Station name	Station code	Station location		Foreshock arrival-times		Main shock arrival-times	
		Latitude	Longitude	*P*	*S*	*P*	*S*
Cape of Good Hope	CAP	33.934S	18.478E	–	–		14 03 00
Göttingen	GOT	51.550N	9.967E	12 03 00	12 13 50	13 56 23	14 03 50
Hamburg	HAM	53.565N	10.022E	12 03 12	12 10 34	13 56 41	14 04 13
Jena	JEN	50.933N	11.583E	12 04 00	12 13 48	13 56 14	14 03 24
Leipzig	LEI	51.335N	12.392E	–	–	–	14 10 30
Mauritius	MAU	20.183S	57.517E	–	–	13 55 30	14 00 30
Osaka	OSA	34.700N	135.517E	–	–	13 58 36	–
Potsdam	POT	52.382N	13.066E	–	–	13 56 26	14 03 34
Rocca di Papa	ROC	41.767N	12.700E	–	–	13 55 29	–
Strasbourg	STR	48.583N	7.769E	12 02 49	12 13 57	13 56 21	14 03 26
Tashkent	TAS	41.325N	69.295E	12 02 11	12 08 00	13 55 29	–
Tiflis	TIF	41.719N	44.798E	–	12 06 12	13 54 20	14 00 38
Trieste	TRI	45.646N	13.763E	12 02 13	–	13 54 39	–
Uccle	UCC	50.798N	4.359E	–	–	–	14 04 31
Uppsala	UPP	59.858N	17.625E	12 03 32	12 11 12	13 56 57	14 04 41
Vienna	VIE	48.248N	16.318E	12 02 18	12 09 09	13 55 54	14 02 36
Zagreb	ZAG	45.815N	15.980E	–	–	13 55 30	–

Table II. Stations used for the waveform data analysis of the three earthquakes. X signifies particular stations used for data analysis of the corresponding event.

Station code	1906/08/25	1910/12/13	1928/01/06
HAM	–	X	–
MNH	–	X	X
UCC	–	X	–
UPP	X	X	X

3.1. *Location and spectral analysis*

Theoretical *S-P* arrival-time differences are calculated for the main shock of the 1906 sequence using the IASPEI-91 travel-time table (Kennett, 1991) for all known previous locations. These are compared with observed arrival-time differences from selected stations (table III). This selection is based on the availability of both *P*- and *S*-phase arrival-time readings. The computation gave consistent results except in a few cases, possibly, due to misidentification of phases.

Generally, absolute value of the residuals in table III decreases from left to right in chronological order, indicating improvement of each location. Most of the travel-time residuals from European stations located in the north are positive. The travel-time residual from the single station in the south (Mauritius) is negative. Such polarisation of the travel-time residual holds true for all locations and for almost all stations, except for Strasbourg where there may be an error in the time correction, and also Tiflis where a clear inconsistency is observed. This is an indication that the epicentre of the 1906 earthquake could be more to the south than all the previously estimated locations. Hence, there is a challenge to relocate this earthquake and its foreshock using the available data summarised in table I.

Table III. Comparison of travel-time residuals for selected stations and all known previous locations.

Observed *S-P* (s)		Calculated *S-P* (s)				Travel-time residual (s)			
Station	Obs. *S-P*	*G & R	†Gouin	×A & A	•A & A	*G & R	†Gouin	×A & A	•A & A
Göttingen	07:25.0	07:03.0	06:55.6	07:10.60	07:14.30	+ 22.0	+ 29.4	+ 14.4	+ 10.7
Hamburg	07:32.0	07:13.0	07:19.6	07:20.50	07:24.00	+ 19.0	+ 12.4	+ 11.5	+ 8.0
Jena	07:10.0	06:55.0	07:00.5	07:03.50	07:07.10	+ 15.0	+ 9.5	+ 6.5	+ 2.9
Mauritius	05:00.0	05:28.2	05:24.3	05:21.50	05:16.00	− 28.2	− 24.3	− 21.5	− 16.0
Potsdam	07:08.0	06:59.8	07:04.7	07:07.60	06:45.00	8.2	+ 3.3	+ 0.4	+ 23.0
Strasbourg	07:00.0	06:55.0	06:59.2	07:02.00	07:06.40	+ 5.0	+ 0.8	− 2.0	− 6.4
Tiflis	06:18.0	05:19.5	05:25.6	05:29.90	05:28.60	+ 58.5	+ 53.4	+ 48.1	+ 51.4
Uppsala	07:44.0	07:32.0	07:37.5	07:40.40	07:42.60	+ 12.0	+ 6.5	+ 3.6	+ 1.4
Vienna	06:42.0	06:30.0	06:24.9	06:37.90	06:31.50	+ 12.0	+ 17.1	+ 4.1	+ 10.5

Following notations represent the various locations: *G & R – by Gutenberg and Richter (1954) from instrumental data (9.0°N, 39.0°E); †Gouin – by Gouin (1979) from macroseismic data (8.0°N, 38.5°E); ×A & A – by Ambraseys and Adams (1991) from macroseismic data (7.5°N, 38.5°E); •A & A – by Ambraseys and Adams (1991) from instrumental data (7.5°N, 40.0°E).

A small-amplitude but almost noise-free waveform dominated by a low frequency signal was recorded on the two horizontal (NS and EW) components at UPP station for the 1906 earthquake (fig. 2). The records show a typical feature of an event due south from the recording station. *PP*, *SS*, and *Lg* phases from Uppsala station were identified and used in the location using the SEISAN software. These additional phases besides *P* and *S* were identified by comparing observed records and synthetic seismograms constructed from a theoretical model of the Earth structure. Generally, differential travel-times of seismic phases (pulses) are used in the location. They are less sensitive to uncertainties than absolute arrival-times. The main shock (7.02°N, 40.09°E) and its foreshock (7.62°N, 40.22°E) are relocated by us on the eastern shoulder of the main Ethiopian rift in line with the southward projection of the N-S trending seismicity pattern of Western Afar (fig. 1).

There is a great deal of uncertainty in the size representation of historical seismicity compiled in different catalogues. This is particularly true for different amplitude-based magnitude scales that saturate at high values and do not take radiation pattern effects into account. The seismic moment, M_0, is the most stable size-rating parameter of earthquakes. M_0 can be obtained from body waves at teleseismic distances using the equation (Udias and Buforn, 1994)

$$M_0 = \frac{4\pi\rho v_j^3 r \exp(\omega r / v_j Q_j)\Omega_0}{c_{j(i_0)} R(\phi, \sigma, \lambda, i_\xi)} \qquad (3.1)$$

where ρ is the density at the focal region, v_j the velocity of *P* or *S* wave at the focal region, the exponential function represents the attenuation of the medium (Q = quality factor), Ω_0 is the spectral amplitude at the flat part of the displacement spectrum of *P* or *S* waves, c is the free surface reflection term and r is distance along the ray path. The procedure requires a good azimuthal coverage of stations about the focal sphere in order to correct for the radiation pattern term $R(\phi,\sigma,\lambda,i_\xi)$. If the radiation pattern term can somehow be controlled, M_0 can be estimated reasonably well at a single station from the flat part of the displacement spectra. This may help to estimate M_0 directly from a few but well recorded seismograms prior to the WWSSN era for large earthquakes in regions where the mode of deformation is well controlled from contemporary geophysical data. The radiation-pattern term at a particular station can be computed from the identified or assumed

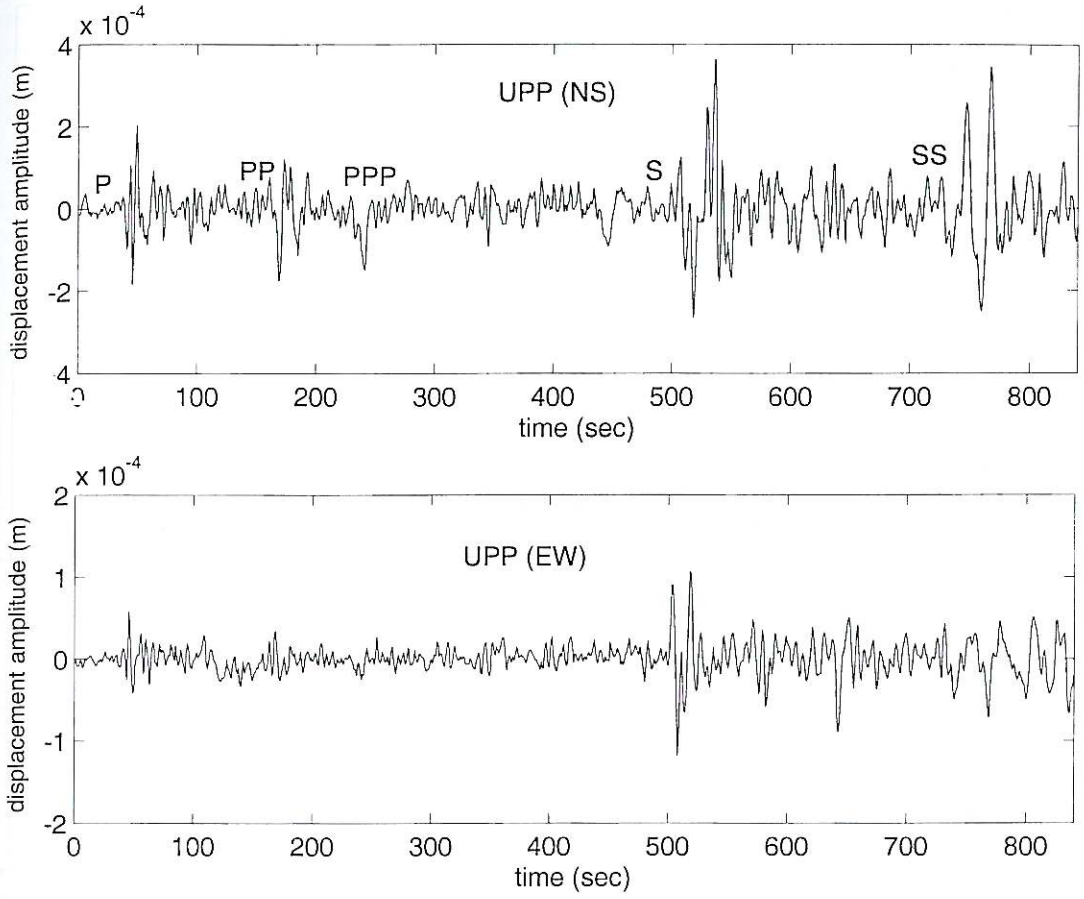

Fig. 2. Body-wave part of seismogram records for the August 25, 1906 earthquake in the main Ethiopian rift. Two horizontal components (NS and EW) made by a Wiechert type instrument at Uppsala.

fault geometry as

$$R(\phi_s,\delta,\lambda) = \cos\lambda\cos\delta\cos i_\xi \sin(\phi\text{-}\phi_s) + \\ + \cos\lambda\sin\delta\sin i_\xi \cos 2(\phi\text{-}\phi_s) + \\ + \sin\lambda\cos 2\delta\cos i_\xi \cos(\phi\text{-}\phi_s) - \\ - 1/2\sin\lambda\sin 2\delta\sin i_\xi \sin 2(\phi\text{-}\phi_s) \quad (3.2)$$

where $(\phi_s, \delta, \lambda)$ = (strike, dip, rake) of the fault, i_ξ is take-off angle, and ϕ is station azimuth (Aki and Richards, 1980). The *SH* wave spectrum after rotation of NS and EW components is used in this study (fig. 3).

3.2. *Waveform inversion for fault mechanism and seismic moment (M_0)*

Long-period *P*- and *SH*-waves from four European stations to the north at teleseismic distances (table II) are inverted for fault mechanisms, source-time functions and seismic moment. The body-wave modelling is performed using the standard procedure developed by Nábelek (1984, 1985) and a crustal model pertinent to the region (Gumper and Pomeroy, 1970). Besides the manual of the IASPEI software (McCaffrey *et al.*, 1991), details are presented by Ayele and Arvidsson (1998). Waveform in-

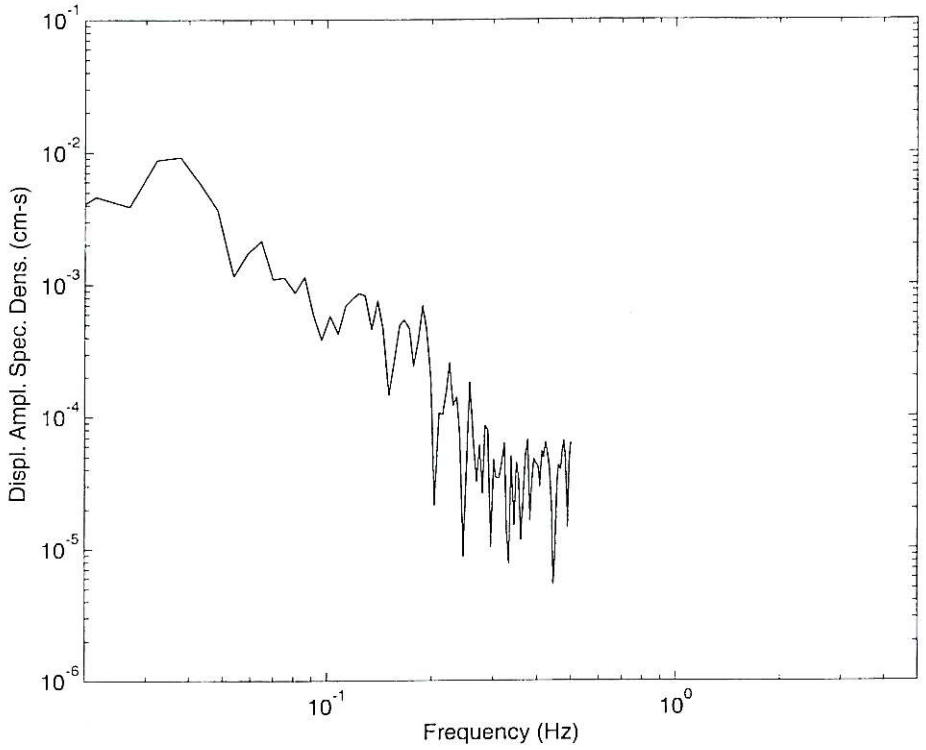

Fig. 3. Displacement spectral plot for the 1906 earthquake from the *SH* wave after rotating the NS and EW components observed at UPP.

version for source parameters is performed for the 1910 and 1928 events (table II).

A preliminary source mechanism was obtained from *P*-wave first-motion study for the 1910 event. The source depth is estimated to be about 16 km from an independent waveform modelling of the vertical component *P*-wave at UCC. The station distribution about the focal sphere was quite poor but a change in polarity was observed from one station to another. This indicates that one of the nodal planes passes through this distribution and hence makes the preliminary fault mechanism result reasonable. This preliminary solution is used as a starting parameter and the depth is fixed to be 16 km in the inversion process. A fair fit between the observed and synthetic waveforms (fig. 4a) is obtained with low variance reduction.

For the 1928 earthquake, good quality records were available only from UPP and MNH, which were not included in the inversion made by Doser and Yarwood (1991). The validity of their result for a significant strike-slip mechanism is tested (fig. 4b) using *P*- and *SH*-waves from the two stations.

4. Results and discussion

The results for earthquake location, spectral analysis and waveform inversion are summarised in table V. The relation $M_w = \log M_0/1.5 - 10.73$ (Kanamori, 1977) is employed in the magnitude conversion. The moment magnitude, M_w, as a measure of earthquake size is free from amplitude saturation problem at high magnitude.

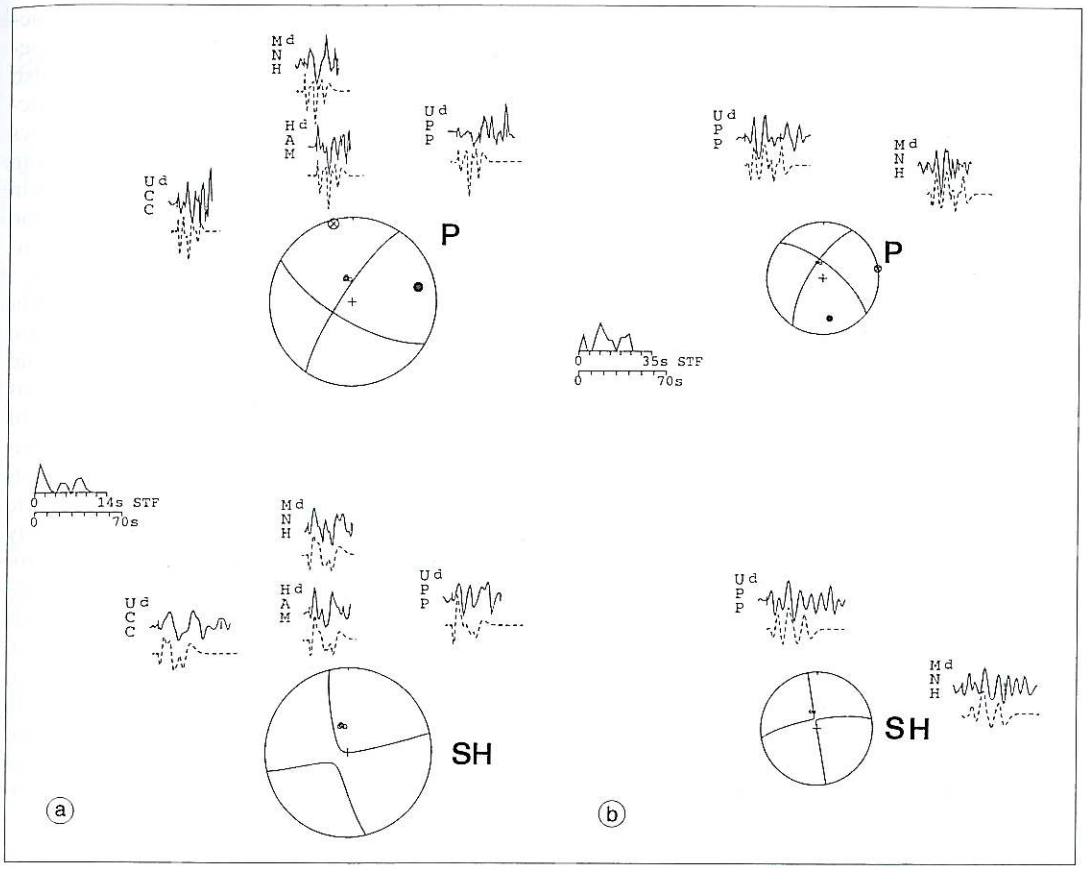

Fig. 4a,b. Focal mechanism (lower hemisphere projection) for the (a) 13/12/1910 and (b) 06/01/1928 earthquakes. Seismogram amplitudes are normalized to their maximum amplitude. Solid traces are observed while dashed traces are synthetic seismograms. In the focal sphere, solid circles are *P* axes while the open circles with an X symbol are *T* axes. Small open circles in the focal sphere represent station distribution. Small letters represent the phase data type: *d* = long-period *P* and *SH* (GDSN). The data are from long-period Wiechert instrument but the instrument response is given in terms of zeroes and poles as if it is a GDSN station, which is required by the program.

Estimating M_w directly from seismograms using contemporary techniques is preferable and more robust than amplitude-based magnitude whenever possible. The corresponding surface wave magnitudes from the Prague formula $M_s = \log(A/T)_{max} + 1.66 \log\Delta + 3.3$ (Vanek *et al.*, 1962) are calculated (table V) from *A*- and *T*-values listed in Uppsala bulletins. Comparing the results obtained in this study with the NEIC (National Earthquake Information Center) catalogue for the East African rift, the 1990 earthquake in Southern Sudan (fig. 5) is the largest of all known events which occurred in East Africa in the instrumental era. This could be due to the fact that Southern Sudan is acting as a pivotal point for different styles of deformation (Girdler and McConnel, 1994). From recent seismicity, Southern Sudan seems to act as a prototype triple junction.

4.1. *The 1906 earthquake sequence in the main Ethiopian rift*

Since we are dealing with historical earthquakes from 1906, the seismicity pattern starting from the turn of this century is displayed in fig. 1 (Gouin, 1979; Ayele, 1995). Most of the earthquakes in Gouin's (1979) catalogue lack magnitude estimates but the location is specified. The same is true in Ayele's (1995) catalogue but the number of events without magnitude is relatively small. A magnitude of 4.0 is assigned for such events prior to 1960 while it is 2.0 for events after 1960 to mark their position on the map. Despite the fact that the main Ethiopian rift is known to be about 100 km wide (Ebinger and Hayward, 1996), the 1906 main event and its foreshock are located outside the rift *i.e.*, on the eastern shoulder of the rift (fig. 1). Gutenberg and Richter (1954) located the epicentres of the two shocks at the same site (9.0°N, 38.7°E), barely 13 km east of Addis Ababa. Gouin (1979) obtained a cluster of intersections nearby (7.5°N, 40.0°E) from instrumental data but this result was given low reliability owing to arrival-time inconsistency. Hence, the location from macroseismic information was the most favoured. The macroseismic data are, however, unreliable due to complication from poorly known timing accuracy in the area and multiple events in the sequence. Site effects and landslides could also considerably influence event locations from macroseismic data even in recent times. Ambraseys and Adams (1991) located the main shock from instrumental data on the eastern side of the main Ethiopian rift (fig. 1), at nearly the same location attempted by Gouin (1979) also from instrumental data but about 50 km north of our location.

Using the Uppsala station bulletin together with records corrected for timing errors helped to filter out the inconsistent station readings and find additional phases from clear seismograms (fig. 2). Considering the possible uncertainty of event locations for that time of data, the instrumental data strongly support the idea that the eastern side of the main Ethiopian rift generated the 1906 sequence. Our attempt made in this study to locate the 1906 earthquake in the main Ethiopian rift from the available bulletins and seismograms gave relatively low travel-time residuals (table IV). This may categorise the 1906 event either as a prototype intraplate earthquake or that the site is in a potentially active seismic region with a long recurrence period for major earthquakes.

No earthquake episode has occurred in that particular area since 1906. The present seismo-

Table IV. Comparison of travel-time residuals for selected stations and all known previous locations with the present study of the 1906 main shock.

	Travel-time residual (s)				
Station	*G & R	†Gouin	×A & A	•A & A	A & K
Göttingen	+ 22.0	+ 29.4	+ 14.4	+ 10.7	+ 8.2
Hamburg	+ 19.0	+ 12.4	+ 11.5	+ 8.0	+ 5.5
Jena	+ 15.0	+ 9.5	+ 6.5	+ 2.9	+ 0.3
Mauritius	− 28.2	− 24.3	− 21.5	− 16.0	− 12.6
Potsdam	8.2	+ 3.3	+ 0.4	+ 23.0	− 5.6
Strasbourg	+ 5.0	+ 0.8	− 2.0	− 6.4	− 8.8
Tiflis	+ 58.5	+ 53.4	+ 48.1	+ 51.4	+ 46.6
Uppsala	+ 12.0	+ 6.5	+ 3.6	+ 1.4	− 0.9
Vienna	+ 12.0	+ 17.1	+ 4.1	+ 10.5	− 2.1

Following notations represent the various locations: *G & R – by Gutenberg and Richter (1954) from instrumental data (9.0°N, 39.0°E); †Gouin – by Gouin (1979) from macroseismic data (8.0°N, 38.5°E); ×A & A – by Ambraseys and Adams (1991) from macroseismic data (7.5°N, 38.5°E); •A & A – by Ambraseys and Adams (1991) from instrumental data (7.5°N, 40.0°E); A & K – by Ayele and Kulhanek for the present study.

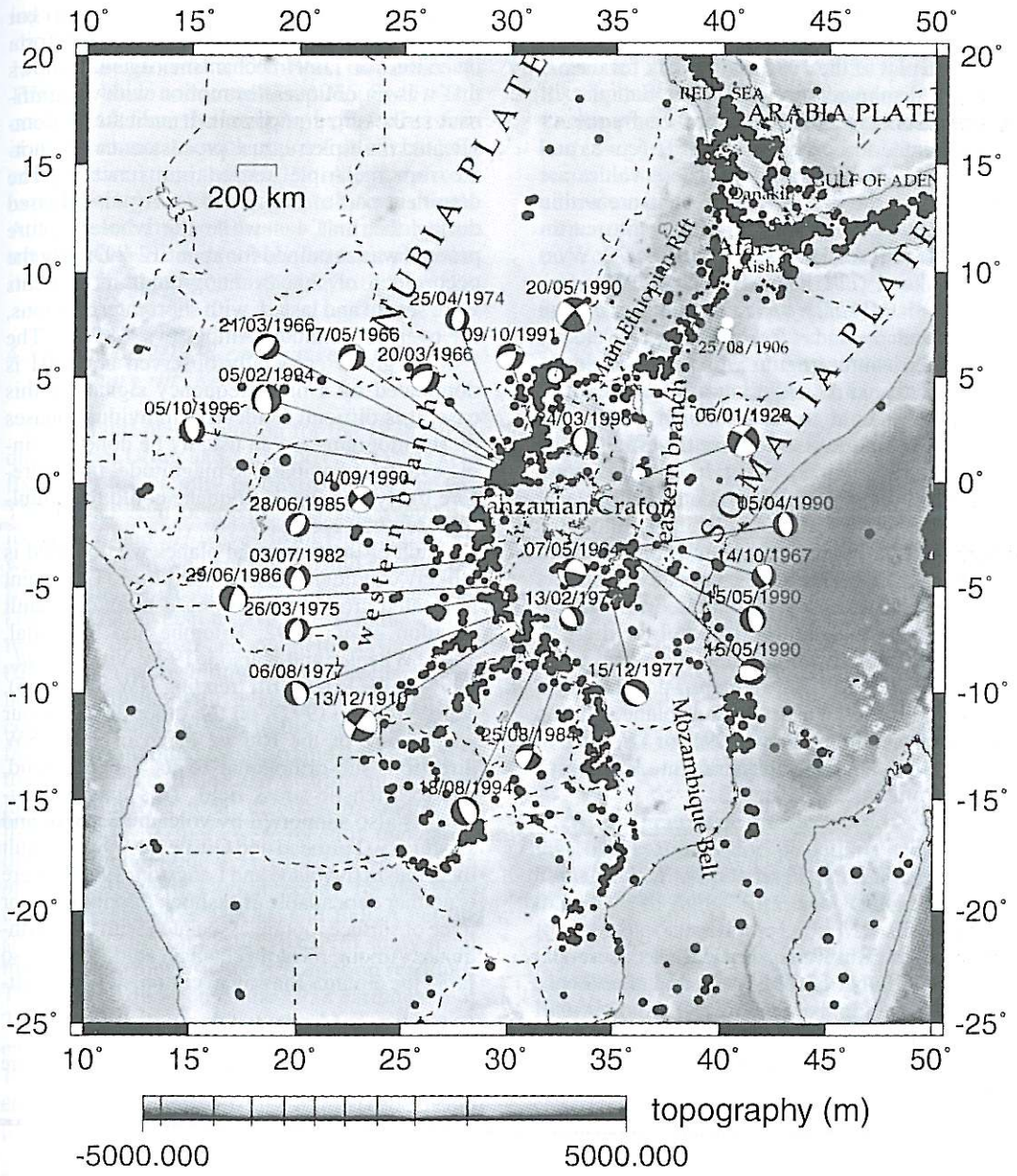

Fig. 5. Seismicity, topography, and focal mechanisms (lower-hemisphere projections) for some events of interest in the East African rift. Except for the 1910 and 1928 events, the other focal mechanisms in the circum-Tanzanian craton are compiled from the CMT catalogue available on the Internet and other previous works referred in the text. The NEIC (National Earthquake Information Center) and Ayele (1995) catalogues from 1973 to present and 1960 to 1993, respectively, are used for the seismicity plot. The white circles are the epicenters of events that are paid special attention in this study. The size of the circles is proportional to magnitude.

graphic network of Ethiopia cannot monitor possible microseismic activity in the area. The spectrum plot of the 1906 main shock for the *SH* wave is displayed in fig. 3. The flat part of displacement spectrum and corner frequency are estimated to be $\Omega_0 = 7.05 \times 10^{-3}$ (cm-s) and $f_0 = 0.044$ (Hz), respectively. These values are picked using the PITSA program and are within the acceptable range for a comparable earthquake magnitude (Hanks and Wyss, 1972; Wyss and Hanks, 1972). From Brune's (1970) relation $r(f_0) = 2.34\beta/2\pi f_0$, a fault radius of 30 km is estimated. β stands for the shear wave velocity around the source region which is 3.55 km/s. The objective of considering as many stations as possible about the source area in spectral analysis technique is to remove the effect of the radiation pattern in eq. (3.2.). In this case, however, good quality waveform data are available only from UPP station. It is likely that this earthquake is related to normal faulting since almost all of the relatively larger earthquakes ($m_b > 5.0$) around this area studied for mechanisms are normal faulting type, following the trend of the main Ethiopian rift (Ayele and Arvidsson, 1998). The radiation-pattern, R, is computed from the average fault-plane solution in the area and found to be 0.091 for *SH*-wave of UPP station. The seismic moment, M_0, is estimated from eqs. (3.1) and (3.2).

4.2. *The 13/12/1910 event in the Rukwa rift (Tanzania)*

The 1910 Rukwa earthquake was accompanied by a number of foreshocks and aftershocks of magnitude $M_s \geq 6.0$ (Ambraseys, 1991a) but with poorly known locations. The waveform inversion for fault mechanism (fig. 4a) shows that it is an oblique-slip motion with a significant strike-slip component. It indicates a complicated multiple rupture process as can be noted from the triple source-time function. The dominant part of the seismic energy is released during the first 4 s while the whole rupture process was sustained for about 12 s. During the occurrence of this event, ground movements were severe and lasted, with short intermissions, for over one minute (Ambraseys, 1991a). The *P*-wave group especially observed at MNH is dominated by a high-frequency signal. In this case, it is difficult to identify individual phases on seismograms as can usually be done for single events of comparable magnitude. It is therefore likely that this earthquake could have multiple ruptures.

Each of the two nodal planes we obtained is a likely candidate to be a fault plane. This event is located around the proposed transform fault (Gaulon *et al.*, 1992; Kilembe and Rosendal, 1992; Wheeler and Karson, 1994; Vittori *et al.*, 1997) in the Rukwa rift trending NW-SE (fig. 5). Morley *et al.* (1992), on the other hand, favour an opening of the Rukwa basin in a NE-SW direction, sub-orthogonal to its general trend, due to a tensile stress field. This line of argument is also supported by volcanic activity and seismicity (Fairhead and Girdler, 1971) and fault mechanism (Nyblade and Langston, 1995). There is neither dependable aftershock distribution nor trace of surface rupture associated with this earthquake. Among focal mechanism studies made so far in the circum-Tanzanian craton, normal fault-

Table V. Source parameters for earthquakes considered in this study. Parameters with standard deviations are the newly computed values.

Date	Origin time (h min s)	Latitude (°N)	Longitude (°E)	Strike (ϕ)	Dip (δ)	Rake (λ)	Depth (km)	M_0 ($\times 10^{19}$ Nm)	M_w	M_s
25/08/1906	11 54 (09±2.2)	7.62±0.4	40.22±0.8	–	–	–	10±8	–	–	5.8
25/08/1906	13 47 (23±1.9)	7.02±0.07	40.09±0.11	–	–	–	15±6	0.74	6.5	6.5
13/12/1910	11 37 30	–7.00	30.03	213±5	79±9	–18±8	16	2.80	6.9	7.0
06/01/1928	19 31 58	0.20	36.20	211±3	70	–158±3	8	1.2	6.6	6.6
20/05/1990	02 22 01	5.07	32.16	321	69	14	13	8.2	7.2	7.2

ing type is dominant but oblique-slip and strike-slip mechanisms are also observed (Shudofsky, 1985; Doser and Yarwood, 1991; Gaulon *et al.*, 1992; Nyblade and Langston, 1995; fig. 5). This could result from the interplay between tensional environment beneath the active rift and the compressive stress that the Pan-African plate is experiencing from the ridge-push forces in the Atlantic and Indian Oceans. The nodal plane trending NW-SE is probably the fault plane but it is still a subject for further investigation.

4.3. *The 06/12/1928 earthquake in the Gregory rift (Kenya)*

The fault plane solution for the 1928 earthquake from Doser and Yarwood (1991) was kept fixed and the validity of this result was tested. The fit between observed data and synthetics for both *P* and *SH* waves from UPP and MNH was poor. Then we kept the dip and focal depth fixed from the results of Doser and Yarwood (1991). The inversion gave a reasonable fit between the observed and synthetic seismograms (fig. 4b). The resulting source mechanism is normal-faulting with a significant strike-slip component striking N-S in the Gregory rift. So far, there is no other event around the vicinity of this earthquake during the instrumental period large enough for focal mechanism studies. In the Gregory rift, there were recently two earthquakes of magnitude 4.3 (April 2, 1996) and 4.5 m_b (April 3, 1996). Digital records for the 1996 events are available at AAE and BGCA but the station distribution is still sparse to study focal mechanism from *P*-wave first-motion readings. The rupture duration of the 1928 earthquake of 26 s is unusually long but possible for this size earthquake (Tajima and Okal, 1997; Kikuchi, 1997) with a multiple rupture where a significant part of seismic energy is released during the occurrence of the second sub-event.

5. Conclusions

The preceding discussion led to the following conclusions:

1) Instrumental data provided evidence for the relocation of the 1906 earthquake sequence in the main Ethiopian rift to be on the eastern side of the active rift. Local seismicity cannot be examined at the moment due to sparse station distribution and poorly known crustal structure. On the other hand, the current seismicity pattern including regional as well as teleseismically recorded shocks shows that the highly populated western side of the rift is more active than the eastern side. This apparent disparity needs serious consideration for seismic hazard assessment and risk mitigation owing to the growing urbanisation especially around Addis Ababa.

2) The NW-SE motion of the southern part of the Somalia plate, relative to the Nubia plate, may remain true but the Tanzanian craton seems to act as a distinct tectonic block sandwiched between the eastern and western branches of the East African rift system. This is inferred from the result of the focal mechanism study of the 1910 and 1928 earthquakes together with previous results of contemporary events. If this detail could be elucidated from a multi-disciplinary aspect, the long awaited question concerning the temporal and spatial relationship between the two branches of the East African rift system might be answered.

Acknowledgements

We are grateful to the directors of seismological observatories for providing seismogram copies and corresponding station bulletins. Our thanks go to Jaime Toral and Ronnie Quintero for valuable discussions; Laike M. Asfaw, Woldai Ghebreab, and Kamal Atiya for reading the manuscript. We thank SIDA/SAREC (Swedish International Development Authority/Swedish Agency for Research Co-operation with Developing Countries) for financial support.

REFERENCES

AKI, K. and P.G. RICHARDS (1980): *Quantitative Seismology: Theory and Methods* (WH Freeman and Co., San Francisco), p. 115.

AMBRASEYS, N.N. (1991a): The Rukwa earthquake of 13 December 1910 in East Africa, *Terra Nova*, **3**, 203-208.

AMBRASEYS, N.N. (1991b): Earthquake in the Kenya rift: the Subukia earthquake 1928, *Geophys. J. Int.*, **105**, 253-269.

AMBRASEYS, N.N. and R.D. ADAMS (1991): Reappraisal of major African earthquakes, south of 20°N, 1900-1930, *Natural Hazards*, **4**, 389-419.

AYELE, A. (1995): Earthquake catalogue of the Horn of Africa for the period 1960-1993, Seismol. Dept. Uppsala Univ., *Report 3-95*, pp. 32.

AYELE, A. and R. ARVIDSSON (1998): Fault mechanisms and tectonic implication of the 1985-87 earthquake sequence in South-Western Ethiopia, *J. Seismol.*, **1**, 383-394.

BRUNE, J.N. (1970): Tectonic stress and the spectra of seismic shear waves from earthquakes, *J. Geophys. Res.*, **75**, 4997-5008.

DOSER, D.I. and D.R. YARWOOD (1991): Strike-slip faulting in continental rifts: examples from Sabukia, East Africa (1928), and other regions, *Tectonophysics*, **197**, 213-224.

EBINGER, C.J. and N.J. HAYWARD (1996): Soft plates and hot spots: views from Afar, *J. Geophys. Res.*, **101**, 21859-21876.

ENGDAHL, E.R. (1997): Applications of re-processed, ISC phase arrival-time data to the construction of reference Earth models, to regional and global tomographic imaging and to seismotectonic studies, in *Abstract in the 29th General Assembly of IASPEI in Thessaloniki (Greece)*, p. 135.

FAIRHEAD, J.D. and R.W. GIRDLER (1971): The seismicity of Africa, *Geophys J. R. Astron. Soc.*, **24**, 271-301.

GAULON, R., J. CHOROWICZ, G. VIDAL, B. ROMANOWICZ and G. ROULT (1992): Regional geodynamic implications of the May-July 1990 earthquake sequence in Southern Sudan, in *Seismology and Related Sciences in Africa*, edited by C.J. EBINGER, H.K. GUPTA and I.O. NYAMBOK, *Tectonophysics*, **209**, 87-103.

GELLER, R.J. and H. KANAMORI (1977): Magnitudes of great shallow earthquakes from 1904 to 1952, *Bull. Seismol. Soc. Am.*, **67**(3), 587-598.

GIRDLER, R.W. and D.A. MCCONNELL (1994): The 1990 to 1991 Sudan earthquake sequence and the extent of the East African rift system, *Science*, **264**, 67-70.

GOUIN, P. (1979): *Earthquake History of Ethiopia and the Horn of Africa*, International Development Research Centre, Ottawa, Ontario, pp. 258.

GUMPER, F. and P.W. POMEROY (1970): Seismic wave velocities and earth structure on he African continent, *Bull. Seismol. Soc. Am.*, **60**, 651-668.

GUTENBERG, B. and C.F. RICHTER (1954): *Seismicity of the Earth and Associated Phenomena* (Princeton University Press, Princeton, N.J.), pp. 273.

HANKS, T. and M. WYSS (1972): The use of body-wave spectra in the determination of seismic-source parameters, *Bull. Seismol. Soc. Am.*, **62** (29), 561-589.

KANAMORI, H. (1977): The energy release in great earthquakes, *J. Geophys. Res.*, **82**, 2981-2987.

KANAMORI, H. (1988): Importance of historical seismograms for geophysical research, in *Historical Seismograms and Earthquakes of the World*, edited by W.H.K. LEE, H. MEYERS and K. SHIMAZAKI (Academic Press, Inc.), pp. 513.

KENNETT, B.L.N. (1991): *IASPEI 1991 Seismological Tables*, Research School of Earth Sciences, Australia National University, Canberra.

KIKUCHI, M. (1997): Size dependence of moment-rate function, in *Abstract in the 29th General Assembly of IASPEI, Thessaloniki (Greece)*, p. 187.

KILEMBE, E.A. and B.R. ROSENDAL (1992): Structure and stratigraphy of the Rukwa rift, *Tectonophysics*, **209**, 143-158.

MCCAFFREY, R., G. ABERS and P. ZWICK (1991): Inversion of teleseismic body waves, in *IASPEI Software Library*, edited by W.H.K. LEE, vol. 3, 81-166.

MORLEY, C.K., S.M. CUNNINGHAMN, R.M. HARPER and W.A. WESCOTT (1992): Geology and geophysics of the Rukwa rift, East Africa, *Tectonics*, **11**, 68-81.

NÁBELEK, J. (1984): Determination of earthquake source parameters from inversion of body waves, *Ph.D. Thesis*, Massachusetts Institute of Technology, Cambridge.

NÁBELEK, J. (1985): Geometry and mechanism of faulting of the 1980 EL Asnam, Algeria, earthquake from inversion of teleseismic body waves and comparison with field observations, *J. Geophys. Res.*, **90**, 12713-12728.

NYBLADE, A.A. and C.A. LANGSTON (1995): East African earthquakes below 20 km depth and their implications for crustal structure, *Geophys. J. Int.*, **121**, 49-62.

RÖGNVALDSSON, S.T. and R. SLUNGA (1993): Routine fault plane solutions for local networks: a test with synthetic data, *Bull. Seismol. Soc. Am.*, **83**, 1232-1247.

SHEDLOCK, K.M., E.R. ENGDAHL and A. VILLASENOR (1997): Earthquake relocation: the ISS catalogue, 1918 through 1942, in *Abstract in the 29th General Assembly of IASPEI in Thessaloniki (Greece)*, p. 391.

SHUDOFSKY, G.N. (1985): Source mechanisms and focal depths of East African earthquakes using Rayleigh-wave inversion and body-wave modelling, *Geophys. J. R. Astron. Soc.*, **83**, 563-614.

TAJIMA, F. and E.A. OKAL (1997): The 1977 three kings ridge earthquake (M_s = 6.7): broardband aspect of the source rupture, *Phys. Earth Planet. Inter.*, **89**, 109-125.

UDIAS, A. and E. BUFORN (1994): Source mechanism of earthquakes from seismic waves, in *2nd Workshop on Three-Dimensional Modeling of Seismic Waves Generation, Propagation and their Inversion, Trieste*.

VALENSISE, G. (1995): Beyond surface faulting: new geological tools for robust assessment of seismic hazard, *Extended Abstract for the International School of Solid Earth Geophysics, Erice-Sicily*.

VANEK, J., A. ZATOPEK, V. KARNIK, N. KONDORSKAYA, Y. RIZNICHENKO, E. SAVARENSKI, S. SOLOVIEV and N. SHEBALIN (1962): Standardization of magnitude scales, *Izv. Acad. Sci. USSR, Geophys. Ser.*, **2**, p. 108.

VITTORI, E., D. DELVAUX and F. KERVYN (1997): Kanda fault: a major seismotectonic element west of the Rukwa rift (Tanzania, East Africa), *J. Geodyn.*, **24**, 139-153.

WHEELER, W.H. and J.A. KARSON (1994): Extension and subsidence adjacent to a «weak» continental transform: an example of the Rukwa rift, East Africa, *Geology*, **22**, 625-628.

WYSS, M. and T. Hanks (1972): The source parameters of San Fernando earthquake inferred from teleseismic body waves, *Bull. Seismol. Soc. Am.*, **62** (29), 591-602.

(received December 15, 1998;
accepted August 20, 1999)